

# $\mathcal{PT}$ -symmetric coupler with a coupling defect: soliton interaction with exceptional point

Yuli V. Bludov<sup>1</sup>, Chao Hang<sup>2</sup>, Guoxiang Huang<sup>2</sup>, and Vladimir V. Konotop<sup>3</sup>

<sup>1</sup>*Centro de Física, Universidade do Minho, Campus de Gualtar, Braga 4710-057, Portugal*

<sup>2</sup>*State Key Laboratory of Precision Spectroscopy and Department of Physics, East China Normal University, Shanghai 200062, China*

<sup>3</sup>*Centro de Física Teórica e Computacional Faculdade de Ciências, Universidade de Lisboa, Instituto para Investigação Interdisciplinar, Avenida Professor Gama Pinto 2, Lisboa 1649-003, Portugal, and Departamento de Física, Faculdade de Ciências, Universidade de Lisboa, Campo Grande, Ed. C8, Piso 6, Lisboa 1749-016, Portugal*

Compiled April 14, 2014

We study interaction of a soliton in a parity-time ( $\mathcal{PT}$ ) symmetric coupler which has local perturbation of the coupling constant. Such a defect does not change the  $\mathcal{PT}$ -symmetry of the system, but locally can achieve the exceptional point. We found that the symmetric solitons after interaction with the defect either transform into breathers or blow up. The dynamics of anti-symmetric solitons is more complex, showing domains of successive broadening of the beam and of the beam splitting in two outwards propagating solitons, in addition to the single breather generation and blow up. All the effects are preserved when the coupling strength in the center of the defect deviates from the exceptional point. If the coupling is strong enough the only observable outcome of the soliton-defect interaction is the generation of the breather.

© 2014 Optical Society of America

OCIS codes: 190.5940,190.6135

Two coupled waveguides (a coupler), with gain and losses which are mutually balanced is a parity-time ( $\mathcal{PT}$ )-symmetric system [1]. In the nonlinear case [2] they represent a testbed for various phenomena involving instabilities and optical solitons. Such couplers support stable propagation of bright [3–5] and dark [6] solitons, breathers [7], and rogue waves [8]. The dynamical properties of these systems are determined by the relation between the strengths of the coupling ( $\kappa$ ) and the gain-loss coefficient ( $\gamma$ ), splitting the region of the parameters in two domains corresponding to the unbroken  $\mathcal{PT}$ -symmetric phase, when all linear modes propagate without amplification or attenuation, and the domain where the linear modes are unstable (the broken  $\mathcal{PT}$ -symmetry). The value of the relation  $\gamma/\kappa$  separating these two domains is an exceptional point (for discussion of physical relevance of exceptional points see e.g. [9]).

When the coupling and gain/loss coefficients changes along the propagation distance, the properties of the medium are affected and new effect can be observed. In particular,  $\mathcal{PT}$ -symmetry with alternating sign can stabilize solitons [4]; a  $\mathcal{PT}$ -symmetric defect with localized gain and loss results in switching solitons between the waveguides [10]. The "governing" ratio  $\gamma/\kappa$  can also be changed by varying the coupling coefficient. This can be done by changing the properties of the medium between the waveguides or by using curved waveguides with varying distance between the waveguides. Such situation was considered for conservative couplers in [11,12], where local change of the coupling constant does not affect qualitatively the properties of the system. In the case of a  $\mathcal{PT}$ -symmetric coupler, however, if change of  $\kappa$  locally reaches (or crosses) the exceptional point the properties

of the coupler are changed qualitatively. In this case the  $\mathcal{PT}$ -symmetric phase is broken locally and one can speak about *exceptional point defect*.

One can expect that if the exceptional point defect is long enough [compared to the wavelength of soliton in the longitudinal direction], a soliton incident on it should become unstable. Indeed, in the spatial domain of the defect, a soliton cannot exist. Then one may expect different scenarios of the soliton instability. These scenarios are addressed in the present Letter. More specifically, we study of the interaction of a vector soliton in a  $\mathcal{PT}$ -symmetric coupler with the localized defect of coupling and report four possibilities of the soliton evolution interacted with the defect: the excitation of a one-period breather, excitation of a breather with oscillating amplitude and width, the splitting of a vector soliton in two breathers, and intensity blowup.

We consider two coupled waveguides described by two nonlinear Schrödinger equations

$$\begin{aligned} i q_{1,z} &= -q_{1,xx} + i\gamma q_1 - \kappa(z)q_2 - |q_1|^2 q_1, \\ i q_{2,z} &= -q_{2,xx} - i\gamma q_2 - \kappa(z)q_1 - |q_2|^2 q_2. \end{aligned} \quad (1)$$

with the coupling  $\kappa = \kappa_0 - (\kappa_0 - \kappa_{min}) e^{-z^2/\ell^2}$ , characterized by the amplitude  $\kappa_0 - \kappa_{min}$  (i.e. it attains the minimal value  $\kappa_{min}$  at  $z = 0$  and tends to  $\kappa_0$  at  $z \rightarrow \pm\infty$ ) and by the width  $\ell$ . To reduce the number of parameters we set  $\gamma = 1$  and leave as the only controlling parameters, the ones describing the coupling defect, i.e.  $\kappa_0$ ,  $\kappa_{min}$  and  $\ell$ . Respectively,  $\kappa_{min} = 1$  corresponds to the exceptional point defect.

In the limiting region where,  $\kappa_{min} \approx \kappa_0$ , Eqs. (1) pos-

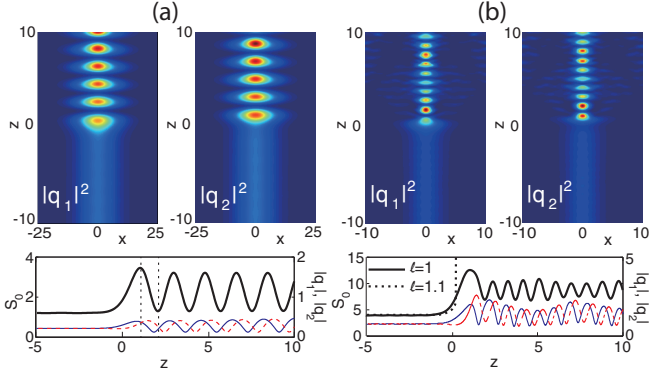


Fig. 1. (color online) Upper panels: Field intensities with (a)  $\eta = 0.15$  and (b)  $\eta = 0.5$  interacting with defect at  $z = 0$ . The coupling  $\kappa_{min} = 1$ ,  $\kappa_0 = 2$  (a) and 4 (b). Lower panels: Respective evolution of the total energy flow  $S_0$  for  $\ell = 1$  [thick solid lines] and soliton amplitudes  $|q_1|$  and  $|q_2|$  [thin solid and dashed lines, respectively]. Thick dotted line in (b) shows blowup at  $\ell = 1.1$ . The local maxima (minima) of  $S_0$  [the vertical lines in lower panel (a)] happen where the powers in the waveguides are equal:  $\int |q_1|^2 dx = \int |q_2|^2 dx$ . The simulations for bounded solutions have been performed between  $z_{ini} = -10$  and  $z_{fin} = 100$  and on the grid  $-40 < x < 40$ .

sess a soliton solution [3]

$$q_1^{(\sigma)} = \frac{\sqrt{2}\eta \exp [i(\eta^2 + \sigma\kappa_0 \cos \delta)z]}{\cosh(\eta x)} = \sigma q_2^{(\sigma)} e^{-i\sigma\delta}, \quad (2)$$

where  $\delta = \arcsin(\gamma/\kappa_0)$  such that  $0 \leq \delta \leq \pi/2$ . The soliton is parametrized by the positive parameter  $\eta$ , and represent symmetric ( $\sigma = 1$ ) and antisymmetric ( $\sigma = -1$ ) solutions. Eq. (2) at  $z = z_{init}$  is used below for the initial data for vector solitons interacting with the defect.

Starting with the interaction of a symmetric soliton ( $\sigma = 1$ ) with the exceptional point defect,  $\kappa_{min} = 1$ , in Fig. 1 we resume the typical results. The figure reveals the two different dynamical scenarios, which depend on whether the length of the defect  $\ell$  is below or above some critical value  $\ell_{cr}$ . In Fig. 1 (a) the soliton passes through a relatively short defect transforming into a breather. The defect width in this case,  $\ell = 1$ , is far below the critical value: for  $\eta = 0.15$ ,  $\kappa_0 = 2$ , and  $\kappa_{min} = 1$  we found  $\ell_{cr} \approx 7$ . The emergent breather solution is characterized by the intensity oscillations between the two components – minimum (maximum) in one component corresponds to maximum (minimum) in the other one [Fig. 1 (a)]. The frequency of these oscillations (after soliton passed the defect) can be estimated as  $2\sqrt{\kappa_0^2 - \gamma^2}$ . For the weakly nonlinear limit this estimate was derived in [7] (it stems from the difference of the eigenfrequencies of the linear  $\mathcal{PT}$ -symmetric coupler). At a finite amplitude the estimate for the frequency can be obtained from the following arguments. Introducing the Stokes variables  $s_0 = |q_1|^2 + |q_2|^2$ ,  $s_1 = q_1 q_2^* + q_1^* q_2$ ,

$s_2 = -i(q_1 q_2^* - q_1^* q_2)$ , and  $s_3 = |q_1|^2 - |q_2|^2$ , as well as their integrals  $S_j = \int_{-\infty}^{\infty} s_j(z, x) dx$ , we obtain

$$\begin{aligned} \frac{dS_0}{dz} &= 2\gamma S_3, & \frac{dS_2}{dz} &= -2\kappa(z)S_3 + \int_{-\infty}^{\infty} s_1 s_3 dx, \\ \frac{dS_1}{dz} &= - \int_{-\infty}^{\infty} s_2 s_3 dx, & \frac{dS_3}{dz} &= 2\gamma S_0 + 2\kappa(z)S_2 \end{aligned}$$

For  $\eta \ll 1$  we have  $\int |q_j|^4 dx \sim \eta^2 \int |q_j|^2 dx$  and  $|\int s_1 s_3 dx| = |\int |q_1|^4 dx - \int |q_2|^4 dx| \ll |S_3|$ . In the case at hand  $\eta = 0.15$  and  $\kappa_0 = 2$  and the nonlinear term in the equation for  $S_2$  can be neglected with the accuracy  $\eta^2/\kappa_0 \approx 0.011$ . As a result the system for  $S_0$ ,  $S_2$  and  $S_3$  become closed and linear. One of its eigenfrequencies is  $2\sqrt{\kappa_0^2 - \gamma^2}$  giving period of oscillations  $\pi/\sqrt{\kappa_0^2 - \gamma^2} \approx 1.8$ ; it agrees well with the numerical results in Fig. 1 (a).

In Fig. 1 (b) the solution passes through the same defect ( $\ell = 1$ ) just below the critical value (for  $\eta = 0.5$ ,  $\kappa_0 = 4$ , and  $\kappa_{min} = 1$  we found  $\ell_{cr} \approx 1.1$ ) and is transformed into a breather. Now the period of oscillations is  $\pi/\sqrt{\kappa_0^2 - \gamma^2} \approx 0.8$ , which still agrees well with the numerical results. The dependencies of the total energy flow  $S_0$  and the solution amplitudes  $|q_{1,2}|$  on  $z$  for each case are shown in the lower panels. When the defect width is close to the threshold value [Fig.1], dependence  $S_0(z)$  becomes quasiperiodic.

In Fig. 2 we show details of the evolution of the Stokes components and phases of the emergent breathers. The breathing character of the mode is evident from almost periodic power imbalance  $S_3$  between the waveguides. We also observe that the breathing solution is accompanied by the oscillation of the "current"  $S_2$  (which is constant for the soliton solution). These oscillations are related to the lifting the phase locking between the components [Fig. 2]: the phase difference  $\theta = \arg q_1 - \arg q_2$ , which is constant for soliton (2), in the breather solution depends periodically on the evolution coordinate. We also confirmed that the Stokes component  $S_1$  remains much smaller than the other ones, what corroborates with the suppositions made in the estimates of the breather period.

If the length of the defect exceeds a critical value  $\ell_{cr}$  for a given coupling constant, the soliton "cannot overcome" it: the component with gain  $q_1$  (and hence  $S_0$ ) grows infinitely. Thus the soliton after passing through the defect blows up [see the dotted line in the lower panel of Fig. 1 (b)]. We performed detail study of the dependence of the critical width of the defect  $\ell_{cr}$  as a function of the minimal coupling  $\kappa_{min}$  [Fig. 3 (a)]. The main qualitative result is that the exceptional point  $\kappa_{min} = 1$  separates quasi-linear (at  $\kappa_{min} < 1$ ) and quasi-exponential (at  $1 < \kappa_{min} < \kappa_{min}^*$ ) dependencies  $\ell_{cr}(\kappa_{min})$ . Interestingly, when  $\mathcal{PT}$ -symmetry is locally broken ( $\kappa_{min} < 1$ ) or even approaches zero, soliton still can pass the coupling defect provided the defect is narrow enough. At the same time, relatively strong coupling prevents blow up: for  $\kappa_{min} > \kappa_{min}^*$  there is no

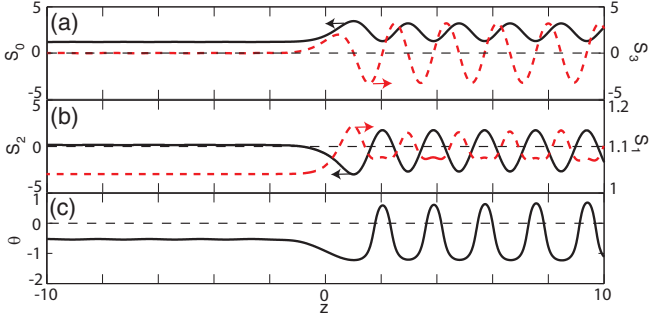


Fig. 2. (color online) (a):  $S_0$  (solid line) and  $S_3$  (dashed line) vs  $z$ ; (b):  $S_2$  (solid line) and  $S_1$  (dashed line) vs  $z$ ; (c):  $\theta$  vs  $z$ . The parameters are the same with those used in Fig. 1 (a).

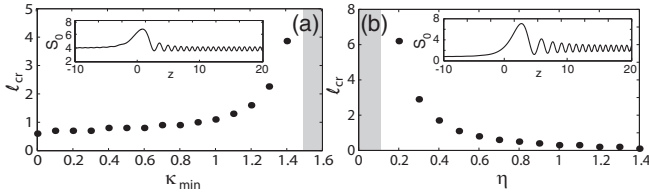


Fig. 3. The dependencies of  $\ell_{cr}$  vs  $\kappa_{min}$  for  $\eta = 0.5$  (a) and vs  $\eta$  for  $\kappa_{min} = 1$  (b). In both panels  $\kappa_0 = 4$ . If  $\kappa_{min} > \kappa_{min}^* \approx 1.5$  (a) and  $\eta < \eta^* \approx 0.1$  (b) (the gray domains) no blow-up is found under the given values of parameters. Insets show the dynamics of Stokes components for a soliton interacting with a strong coupling defect  $\kappa_{min} = 1.5$  (a) and for a small amplitude soliton ( $\eta = 0.1$ ) interacting with the exceptional point defect (b), where sufficiently long defect,  $\ell = 10$ , results in excitation of a breather.

critical width of a defect, and a soliton can pass a defect of *any* width being transformed in a breather. In the inset of Fig. 3 (a) we show an example of strong coupling  $\kappa_{min} = 1.5$ , where the defect with sufficiently long width  $\ell = 10$  results in excitation of breathers. The blow up can occur in the whole interval of weak coupling  $0 < \kappa_{min} < \kappa_{min}^*$  (in Fig. 3 (a),  $\kappa_{min}^* \approx 1.5$ ).

In Fig. 3 (b) we show the dependence of  $\ell_{cr}$  on the inverse soliton width  $\eta$  at  $\kappa_0 = 4$  and  $\kappa_{min} = 1$ . For a given defect width there exist a critical soliton amplitude separating small amplitude solitons which pass the impurity being transformed in breathers and large amplitude solitons which blow up. We also observe an upper critical amplitude  $\eta_{cr}^2 = 2\sqrt{\kappa_0^2 - 1}/3 \approx 1.6$ , above which a soliton blows up independently of the width of the defect. This last effect is a manifestation of the instability of large amplitude solitons in a  $\mathcal{PT}$ -symmetric coupler [3]. Like in the previous case, solitons with  $\eta < \eta^* \approx 0.1$  are able to pass the defect of any width without blow-up. In the inset of Fig. 2 (b) we show an example of excitation of a breather by a small amplitude solitons.

Turning to the interaction of the antisymmetric soliton  $\sigma = -1$  with an exceptional point defect we observe more

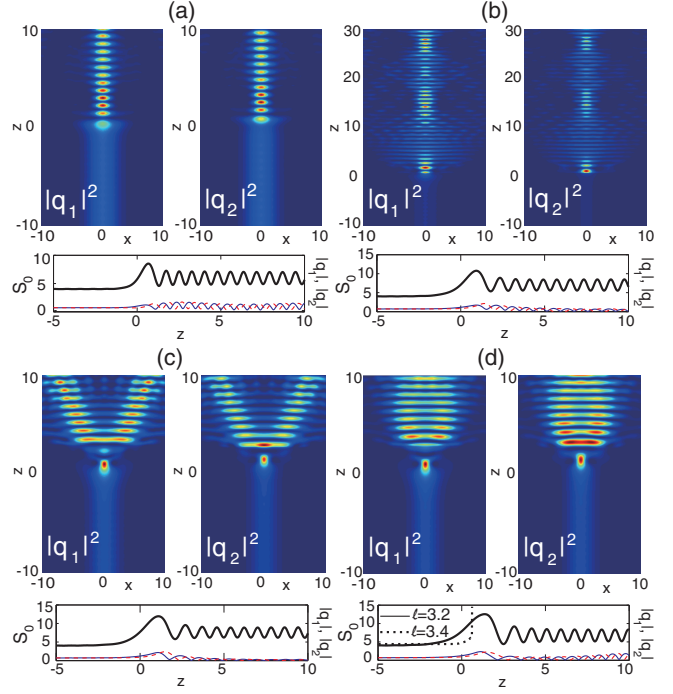


Fig. 4. (color online) Upper panels: The dynamics of soliton-defect interactions for  $\eta = 0.5$  and  $\ell = 1.1$  (a), 2.2 (b), 2.7 (c), and 3.2 (d), respectively, for the coupling  $\kappa_0 = 4$  and  $\kappa_{min} = 1$ . In (a) and (b) The broadening is repeated along the propagation distance with the period  $\approx 10$ . Lower panels: The total energy flow  $S_0$  [thick solid lines] and soliton amplitudes  $|q_1|$  and  $|q_2|$  [thin solid and dashed lines, respectively] for each solution. Thick dotted line in (d) corresponds to the blow up happening at  $\ell = 3.4$ .

rich behavior, which is resumed in Fig. 4. As in the case of symmetric soliton we find that there exists a critical defect length  $\ell_{cr}$  above which the soliton blows up (for the chosen parameters  $\ell_{cr} \approx 3.4$ ). If the width of the defect is below  $\ell_{cr}$ , the soliton-defect interaction results in creation of breathers, although this occurs now according to different scenarios. The effect of a relatively short defect acts similarly on the symmetric and anti-symmetric solitons, c.f. panels (a) in Figs. 1 and 4, here one observes that the antisymmetric breathers have shorter period ( $\approx 0.8$ ) than that of the symmetric ones.

Increase of the defect lengths results in broadening of the soliton passed the defect [Fig. 4 (b)]. This broadening is repeated along the propagation distance [in Fig. 4 (b) the period  $\approx 10$ ]. Further increase of  $\ell$  leads to splitting of the incident soliton in the two outward propagating pulses, as it is shown in Fig. 4 (c). It turns out that the domain of the defect lengths leading to the splitting of the incident beam is finite (for the parameters of Fig. 4 this is the domain  $2.2 \leq \ell \leq 3.2$ ). Interestingly, further increasing of the defect length stops soliton splitting and reintroduces the scenario when broadening of the soliton is observed [Fig. 4 (d)]. In spite of the reported diversity of the behaviors, the total energy flow  $S_0$  is increasing

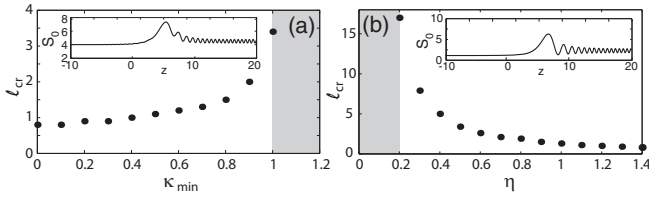


Fig. 5. (a)  $\ell_{cr}$  vs  $\kappa_{min}$  for  $\eta = 0.5$  and (b)  $\ell_{cr}$  vs  $\eta$  for  $\kappa_{min} = 1$ . In both panels  $\kappa_0 = 4$ . If  $\kappa_{min} > \kappa_{min}^* \approx 1$  (a) and  $\eta < \eta^* \approx 0.2$  (b) (the gray domains) no blowup occurs for the given parameters. Insets show the Stokes components for the defect with  $\kappa_{min} = 1.1$  (a) and for the small amplitude soliton ( $\eta = 0.1$ ) interacting with the exceptional point defect (b), where the defect of the length  $\ell = 10$  results in excitation of breathers.

smoothly with the growth of  $\ell$  displaying no reflection of the broadening or splitting dynamics.

In Fig. 5 we show  $\ell_{cr}$  vs  $\kappa_{min}$  [panel (a)] and  $\ell_{cr}$  vs  $\eta$  for  $\kappa_{min} = 1$  [panel (b)] for the case of anti-symmetric soliton. Comparing Figs. 5 and 3 we observe that blowup of a symmetric soliton occurs at lower amplitudes and smaller defect lengths, than the blowup of an anti-symmetric soliton.

Interactions of the solitons with the defect obey several common features. First, soliton-defect interaction starts with the local increase of the energy flow. Indeed, the initial (solitonic) values of the Stokes parameters are given by:  $S_0^{(s)} = 8\eta$ ,  $S_1^{(s)} = 8\eta\sigma \cos \delta$ ,  $S_2^{(s)} = -8\eta \sin \delta$ ,  $S_3^{(s)} = 0$  ( $s_3 \equiv 0$ ) and thus (3) gives that at the initial stage of evolution  $S_0$  and  $S_3$  are growing independently of defect parameters. Second, it follows from (3) that for an *exact* breathing, i.e.  $L$ -periodic, solution  $\langle S_3 \rangle = \frac{1}{L} \int_z^{z+L} S_3(z) dz = 0$ . For a breather far from the defect, where  $\kappa(z) \approx \kappa_0$ , we also find that  $\langle S_2 \rangle = -(\gamma/\kappa)\langle S_0 \rangle < 0$ . Thus, the defect results in oscillations of  $S_2(z)$  without changing the sign of its average.

Finally, using the super-Gaussian defect  $\kappa = \kappa_0 - (\kappa_0 - \kappa_{min}) e^{-z^6/\ell^6}$ , we checked how sensitive are our results to the choice of the defect. We found that for the parameters as in Fig. 1(b) the critical value becomes  $\ell_{cr} \approx 0.5$ . For the antisymmetric mode results are shown in Fig. 6. We do observe that there are the same scenarios, as those in Fig. 4 (although now  $\ell_{cr} \approx 2.3$  for  $\eta = 0.25$ ). It is interesting, that for  $\eta = 0.5$  the critical value  $\ell_{cr} \approx 1.1$ , i.e. considerably lower, than the one established in Fig. 4.

To conclude, we considered interaction of a diffractive soliton in a  $\mathcal{PT}$ -symmetric coupler with a coupling defect, which locally achieves the exceptional point of the underline linear system. Independently on whether the incident beam (soliton) is symmetric or anti-symmetric, at relatively small defect length the soliton passes through the defect and transforms into a breather. This occurs even if in the region of the defect the  $\mathcal{PT}$ -symmetry is broken. If the defect is long enough, the total energy flow grows exponentially along the waveguides. In the case of an anti-symmetric soliton interacting

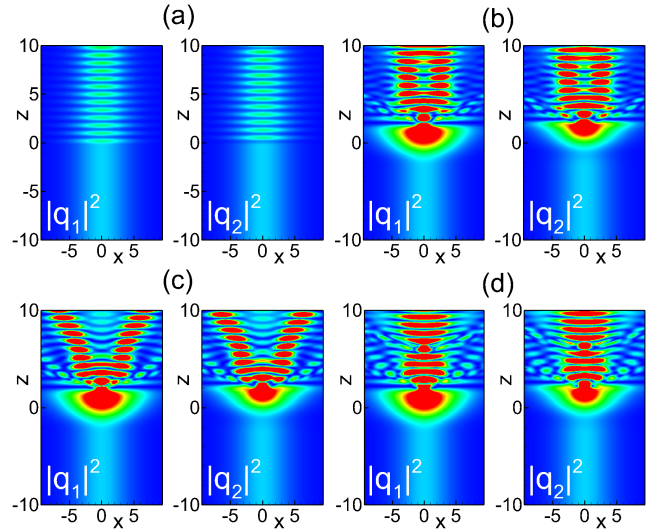


Fig. 6. (color online) Soliton interaction with super-Gaussian defect for  $\eta = 0.25$ ,  $\kappa_0 = 4$ ,  $\kappa_{min} = 1$  and  $\ell = 0.2$  (a);  $\ell = 2.0$  (b);  $\ell = 2.1$  (c);  $\ell = 2.2$  (d).

with a defect there can exist domains where successive broadening of the beam and even beam splitting in two outwards propagating breathers occurs.

The work was supported by the Program of Introducing Talents of Discipline to Universities under Grant No. B12024. YVB and VVK were supported by FCT (Portugal) grants PEst-C/FIS/UI0607/2013, PEst-OE/FIS/UI0618/2011, PTDC/FIS-OPT/1918/2012. CH and GXH were supported by the NSF-China grants 11105052 and 11174080.

## References

1. C. E. Rüter, K. G. Makris, R. El-Ganainy, D. N. Christodoulides, M. Segev, and D. Kip, *Nature Phys.* **6**, 192 (2010).
2. H. Ramezani, T. Kottos, R. El-Ganainy, and D. N. Christodoulides, *Phys. Rev. A* **82**, 043803 (2010).
3. R. Driben and B. A. Malomed, *Opt. Lett.* **36**, 4323, (2011)
4. R. Driben, and B. A. Malomed, *EPL (Europhysics Letters)*, **96**, 51001 (2011)
5. N. V. Alexeeva, I. V. Barashenkov, A. A. Sukhorukov, and Y. S. Kivshar, *Phys. Rev. A* **85**, 063837 (2012)
6. Y. V. Bludov, V. V. Konotop, and B. A. Malomed, *Phys. Rev. A* **87**, 013816 (2013)
7. I. V. Barashenkov, S. V. Suchkov, A. A. Sukhorukov, S. V. Dmitriev, and Y. S. Kivshar, *Phys. Rev. A*, **86**, 053809 (2012)
8. Y. V. Bludov, R. Driben, V. V. Konotop, and B. A. Malomed, *J. Optics*, **15**, 064010 (2013)
9. W. D. Heiss, *J. Phys. A* **45** 44016 (2012).
10. F. K. Abdullaev, V. V. Konotop, M. Öggen, and M. P. Sørensen, *Opt. Lett.*, **36**, 4566 - 4568 (2011).
11. P. L. Chu, B. A. Malomed, G. D. Peng, and I. M. Skinner, *Phys. Rev. E* **49**, 5763 (1994)
12. I. M. Skinner, G. D. Peng, B. A. Malomed, and P. L. Chu, *Opt. Comm.* **113**, 493 (1995)